*Vietnam Journal of Science and Technology* ***58*** *(6) (2020) 776-788*

doi:10.15625/2525-2518/58/6/15298

# MODAL ANALYSIS OF CRACKED TOWER CRANE WITH AN EXPERIMENTAL VALIDATION

**Dang Xuan Trong[1], Le Khanh Toan[2], Ha Thanh Ngoc[3], Nguyen Tien Khiem[2, 3]**

[1]*Occupational Safety and Health Inspection & Training Joint Stock Company*
*733 Xo Viet Nghe Tinh, Ward 26, Binh Thanh Dist., Ho Chi Minh City, Viet Nam*

[2]*Institute of Mechanics, VAST, 264, Doi Can, Ba Dinh, Ha Noi, Viet Nam*

[3]*Institute of Mechanics and Environment Engineering, VUSTA,*
*264 Doi Can, Ba Dinh, Ha Noi, Viet Nam*

[*]Email: *ntkhiem@imech.vast.vn*

Received: 20 July 2020; Accepted for publication: 9 October 2020

**Abstract.** In this paper, dynamic stiffness model of a cracked frame structure that represents a planar tower crane is established in an explicit form based on general solution of cracked 2D-beam element vibration. The crack is modeled by a pair of equivalent springs of stiffness calculated from the crack depth. An explicit form of frequency equation is first established and then solved for numerical sensitivity analysis of natural frequencies of the structure to cracks. An experimental study is accomplished to validate the theoretical development.

*Keywords*: tower crane; cracked structure; modal analysis; dynamic stiffness method.

*Classification numbers*: 5.4.2, 5.4.3.

## 1. INTRODUCTION

Since cranes are indispensable equipment in construction and transportation, dynamic analysis of such the structures is vitally important in both designing and operating stages, especially for the cranes of huge sizes. Dynamic analysis of cranes is required not only to evaluate the dynamic load capacity but also for health monitoring, i. e. checking for integrity of the crane structures. Both the theoretical investigation and practical application of engineering structures demonstrated that vibration-based technique that uses the dynamical characteristics of a structure for accessing its integrity is the most up-to-date fruitful tool for structural damage detection.

The dynamic analysis of cranes was given in various formulations in [1 - 5]. The first model used for dynamic analysis of cranes was simply single degree of freedom systems [1]. Then, the powerful finite element method (FEM) [6 - 8] has been used for dynamic analysis of tower cranes. It has to note that the first effort to apply the FEM dynamic analysis of cranes for their damage identification was accomplished by Wang *et al*. [9]. Nevertheless, the FEM, based on the Hermit's static shape functions, is limited to use for structural dynamic analysis only in low frequency range. This limitation of FEM can be overcome by using the so-called dynamic

stiffness method (DSM) that is one of the exact methods for dynamic analysis of structures in arbitrarily high frequency range.

First effort to develop the DSM for modal analysis of simple tower crane model with a crack was undertaken by the authors in [10]. This study addresses further development of the DSM for modeling dynamics of cracked tower crane. Especially, an experimental study is accomplished to validate the proposed dynamic stiffness model of cracked tower cranes.

## 2. DYNAMIC STIFFNESS MODELING OF CRACKED TOWER CRANE

### 2.1. Dynamic stiffness formulation for cracked beam elements

Let's consider the typical two-node 2D-beam element, axial and vibrations of which according to the classical beam theory are decoupled and described by the different equations

$$\rho A\ddot{u}(x,t) - EAu''(x,t) = 0,\ \rho A\ddot{w}(x,t) + EIw^{(IV)}(x,t) = 0, \tag{2.1}$$

that can be transferred to the form in the frequency domain as

$$U''(x,\omega) + \lambda_u^2 U(x,\omega) = 0;\ W^{(IV)}(x,\omega) - \lambda_w^4 W(x,\omega) = 0,$$
$$\lambda_u = \omega\sqrt{\rho/E};\ \lambda_w = (\rho A\omega^2/EI)^{1/4}, \tag{2.2}$$

where

$$\{U(x,\omega), W(x,\omega)\} = \int_{-\infty}^{+\infty} \{u(x,t), w(x,t)\} e^{-i\omega t} dt.$$

Introducing the complex nodal displacement and forces as shown in Fig. 1 that are defined as

$$U_1(\omega) = U(0,\omega);\ U_2(\omega) = U(\ell,\omega);\ W_1(\omega) = W(0,\omega);\ W_2(\omega) = W(\ell,\omega); \tag{2.3}$$
$$\Theta_1(\omega) = W'(0,\omega);\ \Theta_2(\omega) = W'(\ell,\omega);$$
$$N_1(\omega) = -EAU'(0,\omega);\ N_2(\omega) = -EAU'(\ell,\omega);\ M_1(\omega) = EIW''(0,\omega);\ M_2(\omega) = -EIW''(\ell,\omega); \tag{2.4}$$
$$Q_1(\omega) = -EIW'''(0,\omega);\ Q_2(\omega) = EIW'''(\ell,\omega).$$

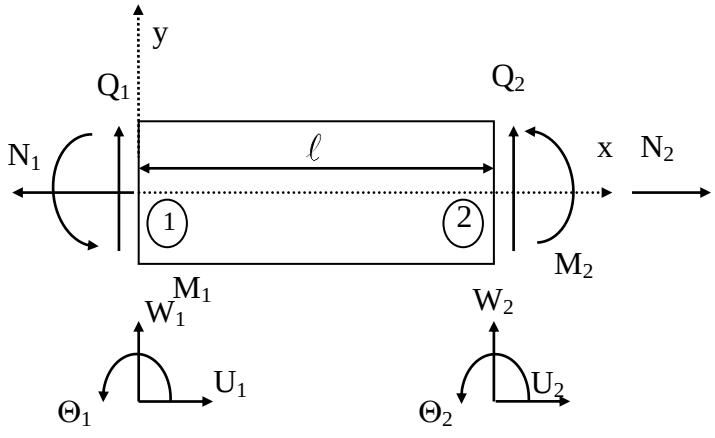


*Figure 1*. Nodal displacements and forces of 2D-beam element in local coordinate system.

Suppose, furthermore, that the element is cracked at positions $e$ with depth $a$ and the crack is modeled by translational (in axial vibration) and torsional (in flexural vibration) springs of stiffness $T$, $K$, calculated from the crack depth (see Appendix 1). In this case, solution of Eq. (2) should satisfy the following conditions at the crack

$$\begin{gathered} U'(e+0)=U'(e-0)=U'(e);U(e+0)=U(e-0)+\gamma U'(e);\gamma_a=EA/T; \\ W(e-0)=W(e+0);W''(e-0)=W''(e+0)=W''(e);W'''(e-0)=W'''(e+0) \\ =W'''(e); \\ W'(e+0)=W'(e-0)+\gamma_b W''(e-0);\gamma_b=EI/R. \end{gathered} \tag{2.5}$$

It was shown in studies by Khiem *et al*., for example, Ref. [11] that general solution of Eq. (22) satisfying conditions (2.5) can be represented in the form

$$\begin{gathered} U(x,\omega)=C_1\phi_1(x)+C_4\phi_4(x); \\ W(x,\omega)=C_2\phi_2(x)+C_3\phi_3(x)+C_5\phi_5(x)+C_6\phi_6(x), \end{gathered} \tag{2.6}$$

where

$$\begin{gathered} \phi_1(x)=\cos\lambda_u x-\lambda_u\gamma\sin\lambda_u e\cdot K_u(x-e),\phi_4(x) \\ =\sin\lambda_u x+\lambda_u\gamma\sin\lambda_u e\cdot K_u(x-e); \\ \phi_2(x)=\sinh\lambda_w x+\lambda_w^2\gamma_b\,cosh\,\lambda_w e\cdot K_w(x-e); \\ \phi_3(x)=\cosh\lambda_w x+\lambda_w^2\gamma_b\,sinh\,\lambda_w e\cdot K_w(x-e); \\ \phi_5(x)=sin\,\lambda_w x-\lambda_w^2\gamma_b\,sin\,\lambda_w e\cdot K_w(x-e); \\ \phi_6(x)=cos\,\lambda_w x-\lambda_w^2\gamma_b\cos\lambda_w e\cdot K_w(x-e); \\ K_u(x)=\begin{cases}0: & x\le 0;\\ \cos\lambda_u x: & x>0;\end{cases} K_w(x)=\begin{cases}0: & x\le 0;\\ S(x): & x>0;\end{cases} S(x)=(sinh\,\lambda_w x+sin\,\lambda_w x)/2\lambda_w. \end{gathered} \tag{2.7}$$

So, putting (2.5) into (2.3) and (2.4) yields

$$\{\boldsymbol{V}(\omega)\}\equiv\begin{Bmatrix}U_1\\W_1\\\Theta_1\\U_2\\W_2\\\Theta_2\end{Bmatrix}=\begin{bmatrix}\phi_1(0) & 0 & 0 & \phi_4(0) & 0 & 0\\ 0 & \phi_2(0) & \phi_3(0) & 0 & \phi_5(0) & \phi_6(0)\\ 0 & \phi_2'(0) & \phi_3'(0) & 0 & \phi_5'(0) & \phi_6'(0)\\ \phi_1(\ell) & 0 & 0 & \phi_4(\ell) & 0 & 0\\ 0 & \phi_2(\ell) & \phi_3(\ell) & 0 & \phi_5(\ell) & \phi_6(\ell)\\ 0 & \phi_2'(\ell) & \phi_3'(\ell) & 0 & \phi_5'(\ell) & \phi_6'(\ell)\end{bmatrix}\cdot\begin{Bmatrix}C_1\\C_2\\C_3\\C_4\\C_5\\C_6\end{Bmatrix}\equiv[\mathbb{Q}]\{\boldsymbol{C}\};$$

$$\begin{aligned}\{\boldsymbol{P}(\omega)\}\equiv\begin{Bmatrix}N_1\\Q_1\\M_1\\N_2\\Q_2\\M_2\end{Bmatrix}&=\begin{bmatrix}-EA\phi_1'(0) & 0 & 0 & -EA\phi_4'(0) & 0 & 0\\ 0 & -EI\phi_2'''(0) & -EI\phi_3'''(0) & 0 & -EI\phi_5'''(0) & -EI\phi_6'''(0)\\ 0 & EI\phi_2''(0) & EI\phi_3''(0) & 0 & EI\phi_5''(0) & EI\phi_6''(0)\\ EA\phi_1'(\ell) & 0 & 0 & EA\phi_4'(\ell) & 0 & 0\\ 0 & EI\phi_2'''(\ell) & EI\phi_3'''(\ell) & 0 & EI\phi_5'''(\ell) & EI\phi_6'''(\ell)\\ 0 & -EI\phi_2''(\ell) & -EI\phi_3''(\ell) & 0 & -EI\phi_5''(\ell) & -EI\phi_6''(\ell)\end{bmatrix}\cdot\begin{Bmatrix}C_1\\C_2\\C_3\\C_4\\C_5\\C_6\end{Bmatrix}\\ &\equiv[\mathbb{R}]\{\boldsymbol{C}\};\end{aligned}$$

Therefore, ignoring vector $\{\boldsymbol{C}\}$ from the latter equations we have got

$$\{\boldsymbol{P}(\omega)\}=[\mathbb{R}][\mathbb{Q}]^{-1}\{\boldsymbol{V}(\omega)\}=[\mathbf{D}(\omega)]\{\boldsymbol{V}(\omega)\}, \tag{2.8}$$

where $\{\boldsymbol{P}(\omega)\}$, $\{\boldsymbol{V}(\omega)\}$ are nodal force and displacement vectors respectively and matrix

$$[\mathbf{D}(\omega)]=[\mathbb{R}][\mathbb{Q}]^{-1} \tag{2.9}$$

is so-called dynamic stiffness matrix of the 2D-beam element in local coordinate system. Letting the nodal force and displacement vectors on global coordinate system be denoted by $\{\widehat{\boldsymbol{P}}(\omega)\}$, $\{\widehat{\boldsymbol{V}}(\omega)\}$ that are related to the local ones by

$$\{\hat{\boldsymbol{P}}(\omega)\} = [\mathbf{T}]\{\boldsymbol{P}(\omega)\}, \{\hat{\boldsymbol{V}}(\omega)\} = [\mathbf{T}]\{\boldsymbol{V}(\omega)\},$$

one gets

$$\{\hat{\boldsymbol{P}}(\omega)\} = [\mathbf{T}][\mathbf{D}(\omega)][\mathbf{T}]^{-1}\{\hat{\boldsymbol{V}}(\omega)\} = [\hat{\mathbf{D}}(\omega)]\{\hat{\boldsymbol{V}}(\omega)\} \quad (2.10)$$

with matrix $[\hat{\mathbf{D}}(\omega)] = [\mathbf{T}][\mathbf{D}(\omega)][\mathbf{T}]^{-1}$ so-called global dynamic stiffness matrix of the beam element.

### 2.2. Dynamic stiffness model of cracked tower crane

Let's now consider free vibration a tower crane shown in Fig. 2. Its model consists of four 2D beam elements {E1, E2, E3, E4}; two bar elements {E5, E6} and 4 nodes {N1,…,N4} with concentrated masses $m_i$ produce the concentrated forces $-m_i\omega^2 U$,$-m_i\omega^2 W$ at nodes.

Global nodal displacement vector of the total structure

$$\{\hat{V}_1, \hat{V}_2, \ldots, \hat{V}_{12}\} = \{U_1, W_1, \Theta_1, \ldots, U_4, W_4, \Theta_4\}.$$

is defined as shown in Fig. 3. Relation between the global displacement vector and the local ones of the crane elements is given in Table 1.

*Table 1.* Definition of global displacement vector of the crane elements.

| Local displacement | Axial-1 | Bending-1 | Slope-1 | Axial-2 | Bending-2 | Slope-2 |
|---|---|---|---|---|---|---|
| Element E1 | 0 | 0 | 0 | $V_1$ | $-U_1$ | $\Theta_1$ |
| E2 | $U_1$ | $V_1$ | $\Theta_1$ | $U_2$ | $V_2$ | $\Theta_2$ |
| E3 | $V_1$ | $-U_1$ | $\Theta_1$ | $V_3$ | $-U_3$ | $\Theta_3$ |
| E4 | $U_4$ | $V_4$ | $\Theta_4$ | $U_1$ | $V_1$ | $\Theta_1$ |
| E5 | $U_{51}$ | 0 | 0 | $U_{52}$ | 0 | 0 |
| | $U_{51} = U_4\cos\alpha_{45} + V_4\sin\alpha_{45}$, $U_{52} = U_3\cos\alpha_{45} + V_3\sin\alpha_{45}$ | | | | | |
| E6 | $U_{61}$ | 0 | 0 | $U_{62}$ | 0 | 0 |
| | $U_{61} = U_3\cos\alpha_{26} - V_3\sin\alpha_{26}$, $U_{62} = U_2\cos\alpha_{26} - V_2\sin\alpha_{26}$ | | | | | |

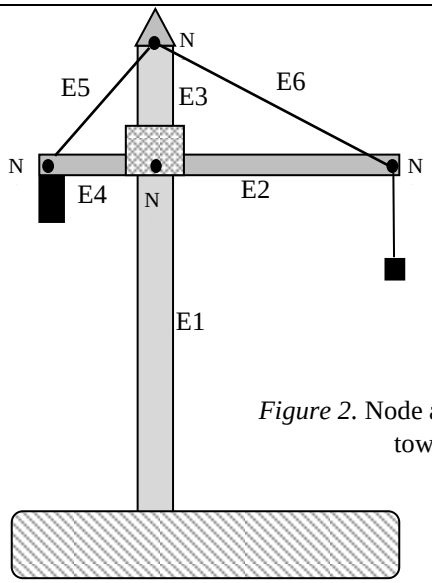


*Figure 2.* Node and element model of tower crane.

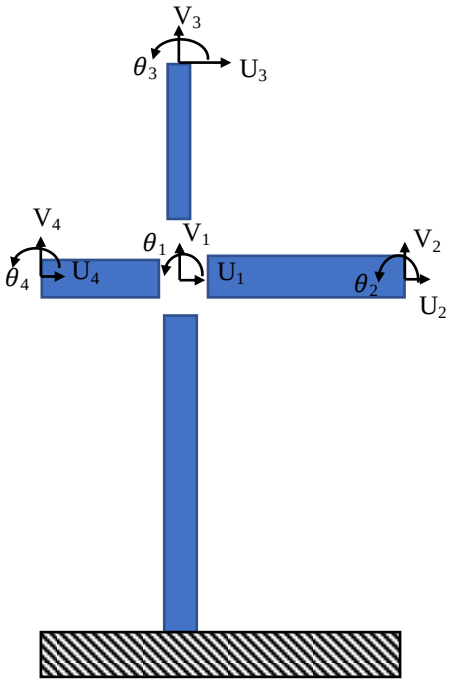


*Figure 3*. Global displacement vector of tower crane.

Furthermore, nodal force vector of all the crane elements are shown in Fig. 4 and all the nodal forces of the entire structure can be calculated by using the relationship (2.10). Balancing all the forces at every node gives rise the equation

$$[\mathbf{K}(\omega)]\{\widehat{\boldsymbol{V}}(\omega)\} = 0, \tag{2.11}$$

where matrix

$$\mathbf{K}(\omega) = \begin{bmatrix} K_{11} & 0 & K_{13} & K_{14} & 0 & 0 & K_{17} & 0 & K_{19} & K_{1,10} & 0 & 0 \\ 0 & K_{22} & K_{23} & 0 & K_{25} & K_{26} & 0 & 0 & 0 & 0 & K_{2,11} & K_{2,12} \\ K_{31} & K_{32} & K_{33} & 0 & K_{35} & K_{36} & K_{37} & 0 & K_{39} & 0 & K_{3,11} & K_{3,12} \\ K_{41} & 0 & 0 & K_{44} & K_{45} & 0 & K_{47} & K_{48} & 0 & 0 & 0 & 0 \\ 0 & K_{52} & K_{53} & K_{54} & K_{55} & K_{56} & K_{57} & K_{58} & 0 & 0 & 0 & 0 \\ 0 & K_{62} & K_{63} & 0 & K_{65} & K_{66} & 0 & 0 & 0 & 0 & 0 & 0 \\ K_{71} & 0 & K_{73} & K_{74} & K_{75} & 0 & K_{77} & K_{78} & K_{79} & K_{7,10} & K_{7,11} & 0 \\ 0 & K_{82} & 0 & K_{84} & K_{85} & 0 & K_{87} & K_{88} & 0 & K_{8,10} & K_{8,11} & 0 \\ K_{91} & 0 & K_{93} & 0 & 0 & 0 & K_{97} & 0 & K_{99} & 0 & 0 & 0 \\ K_{10,1} & 0 & 0 & 0 & 0 & 0 & K_{10,7} & K_{10,8} & 0 & K_{10,10} & K_{10,11} & 0 \\ 0 & K_{11,2} & K_{11,3} & 0 & 0 & 0 & K_{11,7} & K_{11,8} & 0 & K_{11,10} & K_{11,11} & K_{11,12} \\ 0 & K_{12,2} & K_{12,3} & 0 & 0 & 0 & 0 & 0 & 0 & 0 & K_{12,11} & K_{12,12} \end{bmatrix} \tag{2.12}$$

with the elements given in Appendix 2. Therefore, natural frequencies $\omega_1, \omega_2, \omega_3, \ldots$ are roots of the equation

$$\det[\mathbf{K}(\omega)] = 0\,, \tag{2.13}$$

with respect to $\omega$.

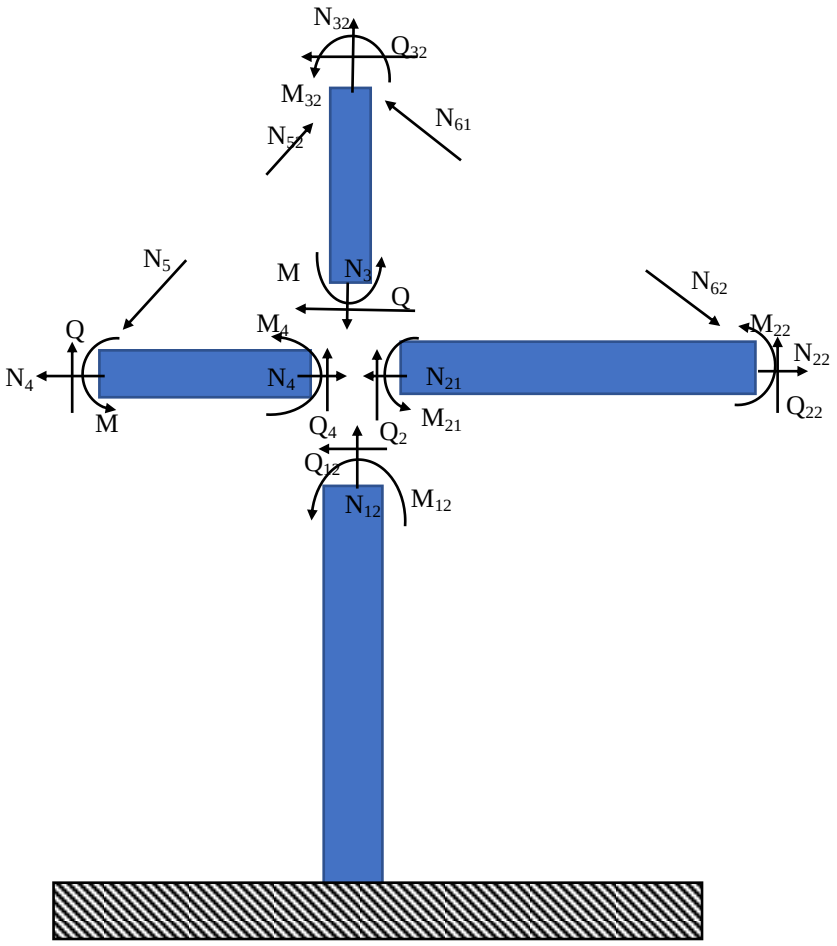


*Figure 4.* Nodal forces defined for all nodes of the crane elements.

## 3. SENSITIVITY OF NATURAL FREQUENCIES TO CRACK

For illustration of the presented above theory, a numerical analysis of first three natural frequencies of a crane with the material and geometry parameters given in Table 2. First, variation of three lowest natural frequencies caused by single crack at every element is examined along the crack position for various depth. The frequencies computed for crack of zero depth are known as natural frequencies of the intact (uncracked) structure. The ratios of natural frequencies of cracked to uncracked structure or otherwise called normalized frequencies are computed and results are presented in Figs. 5 - 7.

The numerical results show that first and second frequencies of the crane are significantly changed by crack at the position on the column closed to cabin (node N1) and the third frequency gets maximum reduction when crack appeared at the column middle (Fig. 5). It can be seen also that there exists position on the column, crack appeared at which makes no effect on the natural frequencies, such the positions are called crack node of a given frequency. Graphics given in Fig. 6 show that crack at the right end of the arm, like the free end of a cantilever, makes a small change in natural frequencies of the crane and the crack node exists on this arm only for third frequency.

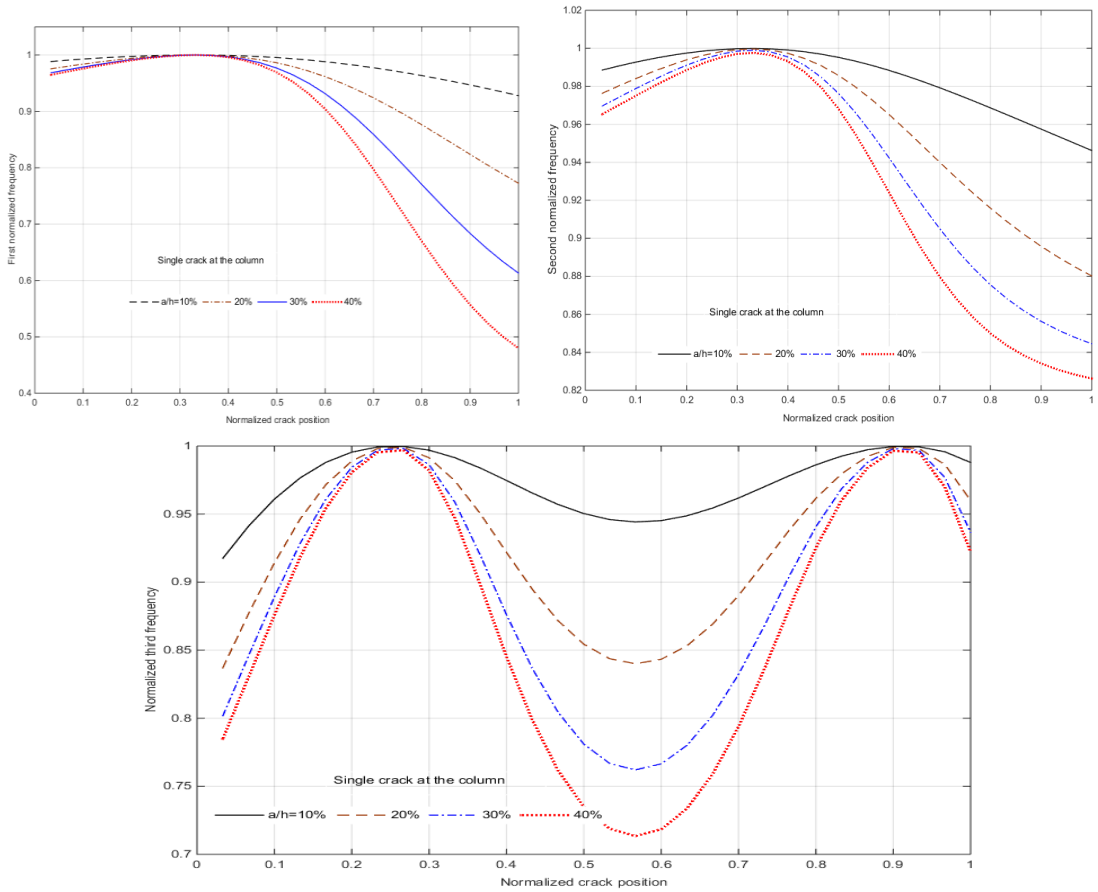


*Figure 5.* Variation of first three natural frequencies caused by a crack at various position on first element.

*Table 2.* Material and geometrical parameters of crane.

| Parameters | Element 1 | Element 2 | Element 3 | Element 4 | Element 5 | Element 6 |
|---|---|---|---|---|---|---|
| E ($N/m^2$) | 2.0e11 | 2.0e11 | 2.0e11 | 2.0e11 | 2.0e11 | 2.0e11 |
| $\rho$ ($kg/m^3$) | 7850 | 7850 | 7850 | 7850 | 7850 | 7850 |
| *b* (m) | 0.03 | 0.008 | 0.028 | 0.008 | - | - |
| *h* (m) | 0.02 | 0.016 | 0.018 | 0.016 | - | - |
| *L* (m) | 44 | 60 | 5.6 | 16 | 17 | 60.3 |
| *R* (m) | - | - | - | - | 0.00075 | 0.00075 |
| Concentrated masses (kg) at nodes 1, 2 and 4: $m_1 = 0.3$; $m_2 = 1.0$; $m_4 = 9.0$ | | | | | | |

Change in natural frequencies of the crane are monotonically increasing as crack moving from counterbalance mass to the cabin position (Fig. 7). As usually, increasing depth of crack leads to more reduction of natural frequencies of the crane. This numerical analysis provides a useful indication for crack detection in crane structure by measurement of natural frequencies.

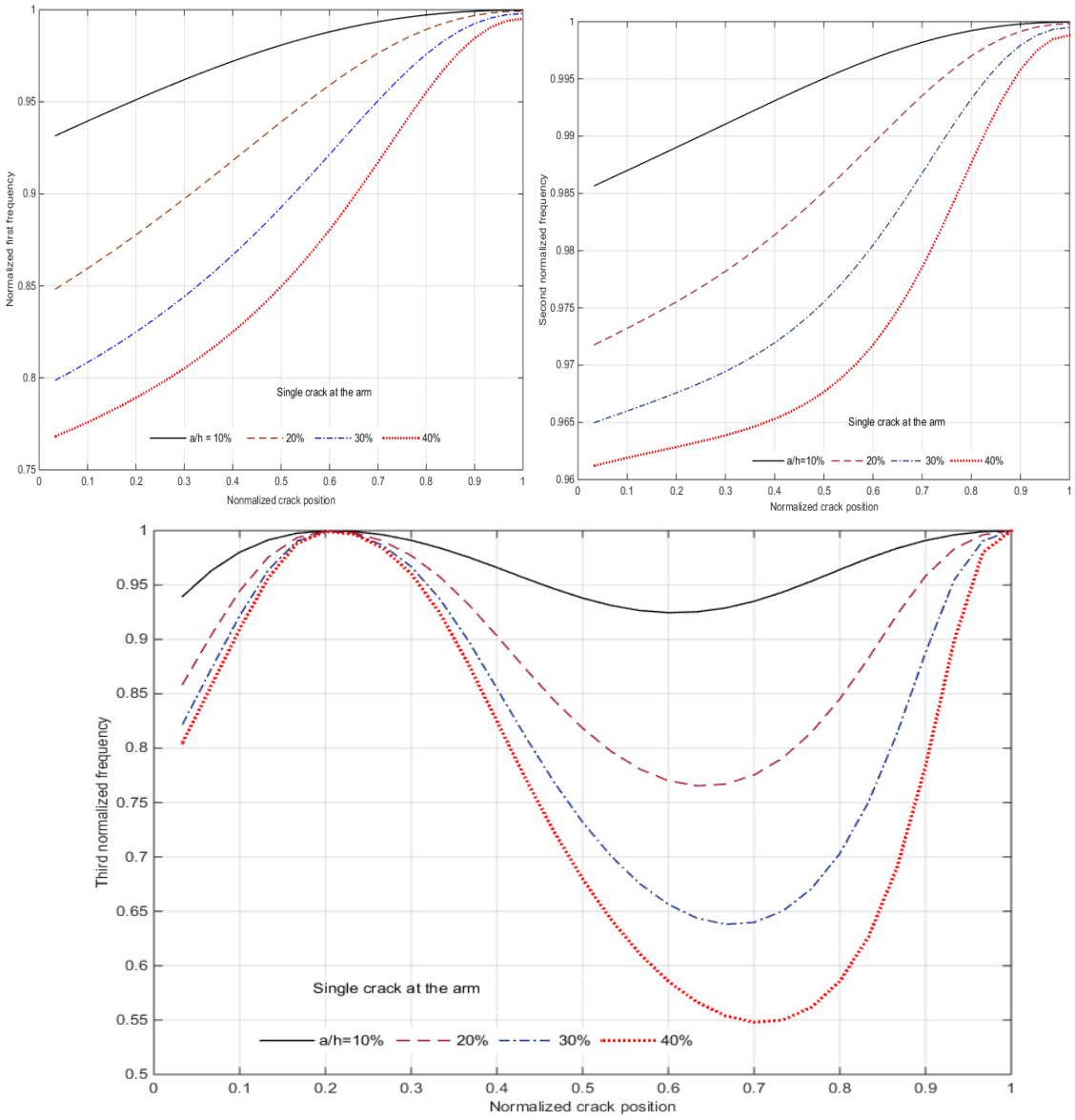


*Figure 6.* Variation of first three natural frequencies caused by a crack at various position on second element.

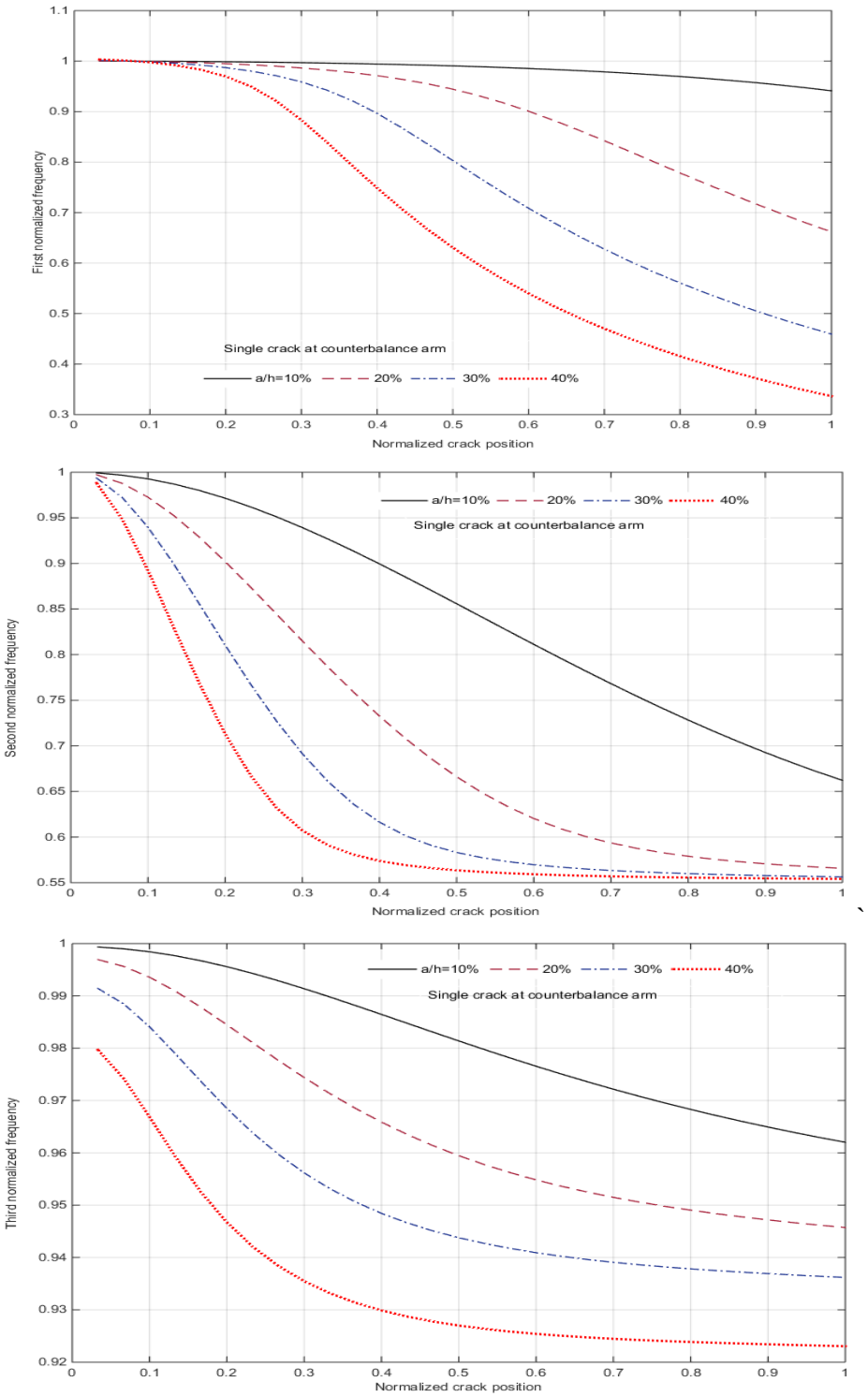


*Figure 7*. Variation of first three natural frequencies caused by a crack at various position on fourth element.

## 4. EXPERIMENTAL VALIDATION

*Table 3.* Comparison of computed and measured natural frequencies of multiple cracked crane structure.

| Crack depth scenarios | First frequency | | Second frequency | | Third frequency | |
|---|---|---|---|---|---|---|
| | DSM | Experiment | DSM | Experiment | DSM | Experiment |
| Undamaged structure | | | | | | |
| 0 % | 18.5866 | **18.47** | 35.5896 | **35.28** | 177.5291 | **176.9** |
| Single crack at column (E1) | | | | | | |
| 10 % | 18.1512 | **18.04** | 34.8265 | **34.69** | 171.0326 | **170.4** |
| 20 % | 17.1214 | **17.08** | 33.3943 | **33.13** | 158.8484 | **158.65** |
| 30 % | 15.8677 | **15.31** | 32.1281 | **31.59** | 148.9218 | **148.25** |
| 40 % | 14.6659 | **14.57** | 31.2195 | **30.94** | 142.3194 | **141.8** |
| Two cracks at column (E1) and arm (E2) | | | | | | |
| 40 % +10 % | 14.4433 | **14.35** | 30.5906 | **30.32** | 140.2371 | **139.74** |
| 40 % +20 % | 13.9862 | **13.89** | 29.4925 | **29.23** | 136.197 | **135.71** |
| 40 % +30 % | 13.5174 | **13.43** | 28.5778 | **28.32** | 132.604 | **132.13** |
| 40 % +40 % | 13.1085 | **13.02** | 27.9151 | **27.5** | 130.0592 | **129.25** |
| Three cracks at column, arm and counterbalance arm (E4) | | | | | | |
| 40 % + 40 % +10 % | 12.9463 | **12.83** | 25.1252 | **24.9** | 124.1505 | **123.7** |
| 40 % + 40 % + 20 % | 12.3941 | **12.31** | 20.6883 | **20.35** | 116.7653 | **116.1** |
| 40 % + 40 % + 30 % | 11.2207 | **10.94** | 17.6675 | **16.72** | 111.9149 | **111.15** |
| 40 % + 40 % + 40 % | 9.5071 | **9.44** | 16.2456 | **16.035** | 107.9844 | **107.07** |

An experiment has been accomplished to validate the theory proposed above. The experimental model is fabricated exactly as shown in Fig. 2 with detailed data given in Table 2. Using the measurement system PULSE 386 including an impact hammer and accelerometer and modal testing technique three lowest natural frequencies have been measured for various scenarios of the cracked crane model [12]. Cracks are made as saw cut of different depth (10 - 20 - 30 - 40 %) at the chosen positions on three main beam elements E1 (at position 472 mm from clamped end), E2 (at position 210 mm from cabin on the left) and E4 (at position 70 mm from cabin on the right). The measurement began from the intact (uncracked) condition of the structure and measured natural frequencies have been acknowledged as baseline data to normalize the frequencies of cracked structure. The measured natural frequencies are compared to those computed by the dynamic stiffness method (DSM) for the experimental model and the comparison is shown in Table 3. After updating in computational model, the difference between measured and computed frequencies is within 5 %, so that the dynamic stiffness model of the crane with cracks is thus experimentally validated.

## 5. CONCLUSION

So, in the present paper, the dynamic stiffness matrix for a typical tower crane is established in an explicit form. This dynamic stiffness model has been used for numerical analysis of natural frequencies of the crane in dependence on the position and depth of crack appeared at every structural element. The theoretical development was validated by an

experiment that shows validity of using both the theoretical model and experimental technique for crack detection of tower crane by measured natural frequencies.

***Acknowledgement:*** This study has been completed with support from the Vietnam National Foundation for Science and Technology Development (NAFOSTED) under Grant Number 107.01-2019.312, to whom the authors are sincerely thankful.

## REFERENCES

1. Abdel-Rahman E.M., Nayfeh A.H. and Masoud, Z.N. - Dynamics and Control of Cranes. A Review. Journal of Vibration and Control **9** (7) (2003) 863-909.
2. Nasser M.A. - Dynamic Analysis of Cranes. Proc. IMAC XIX, paper No. 194301, pp. 1592-1599.
3. Oguamanam D.C.D. and Hansen J.S. - Dynamic response of an overhead crane system. Journal of Sound and Vibration **243** (5) (1998) 889-906.
4. Ghigliazza R.M. and Holmes P. - On the Dynamics of Cranes or Spherical Pendula with Moving Supports. Intern. J. of Nonlinear Mechanics **37** (6) (2002) 1211-1221.
5. Eden J.F., Homer P. and Butler A.J. - The Dynamic Stability of Mobile Cranes. Proceedings of the Institution of Mechanical Engineers, Part D: Journal of Automobile Engineering **199** (D4) (1985) 283-293.
6. Ju F. and Choo Y.S. - Dynamic characteristics of tower cranes. Proc. 2nd Int. Conf. on Structural Stability and Dynamics. World Scientific, Singapore (2002) 260-266.
7. Ju F. and Choo Y.S. - Dynamic Analysis of Tower Cranes. Journal of Engineering Mechanics **131** (1) (2005) 88-96.
8. Ju F., Choo Y.S. and Cui F.S. - Dynamic response of tower induced by the pendulum motion of the payload. International Journal of Solids and Structures **43** (2) (2006) 376-389.
9. Wang S., Shen R., Jin T. and Song S. - Dynamic Behavior Analysis and Its Application in Tower Crane Structure Damage Identification. Advanced Materials Research **368-373** (2012) 2478-2482.
10. Khiem N.T., Trong D.X. - Modal Analysis of Tower Crane with Cracks by the Dynamic Stiffness Method. Topics in Modal Analysis & Testing, Volume 10, Chapter 2, 2017, 11-22. M. Mains, J.R. Blough (eds.)
11. Khiem N.T., Tran T.H. - A procedure for multiple crack Identification in beam-like structures from natural vibration mode. Journal of Vibration and Control **20** (9) (2014) 1417-1427.
12. Nguyen Tien Khiem. Introduction to Experimental Mechanics, VNU Publishing House, Hanoi, 2012.

## NOMENCRATURE

$L, b, h$ – Length, wideness, thickness of beam

$A = bh, I = bh^3/12$ - Cross section area and moment of inertia

$E, \rho$ - Modulus of elasticity and mass density

$u_0(x,t); w_0(x,t)$ – Axial and flexural displacements at the neutral plane of beam

$T$, $R$ – Stiffness of translational and torsional springs representing a crack

$\gamma_a = EA/T$; $\gamma_b = EI/R$ - Crack magnitudes (axial and flexural)

$\alpha_{26}$; $\alpha_{45}$ - Angles between elements 2 and 6 and elements 4 and 5

$h_{1k}(x)$; $h_{2k}(x)$ - Dynamic shape functions for axial vibration of *k*-th element

$H_{1j}(x), H_{2j}(x), H_{13}(x), H_{4j}(x)$ - Dynamic shape functions for bending vibration of *j*-th element

## APPENDIX 1

### Formulas for calculation of crack magnitude from crack depth

$$\gamma = E_0 A / T = 2\pi(1-\nu_0^2) h f_u(z), z = a/h; \tag{A1.1}$$

$$f_u(z) = z^2(0.6272 - 0.17248\,z + 5.92134\,z^2 - 10.7054\,z^3 + 31.5685\,z^4 - 67.47\,z^5 + \\ + 139.123\,z^6 - 146.682\,z^7 + 92.3552\,z^8);$$

$$\theta = EI/R = 6\pi(1-\nu_0^2) h f_w(z); \tag{A1.2}$$

$$f_w(z) = z^2(0.6272 - 1.04533\,z + 4.5948\,z^2 - 9.9736\,z^3 + 20.2948\,z^4 - 33.0351\,z^5 + \\ + 47.1063\,z^6 - 40.7556\,z^7 + 19.6z^8).$$

## APPENDIX 2

### Elements of the dynamic stiffness for crane

$K_{11} = -EA_2h'_{11}(0) - EI_1H'''_{31}(\ell_1) + EA_4h'_{24}(\ell_4) + EI_3H'''_{13}(0) - m_1\omega^2$; $K_{13} = EI_1H'''_{41}(\ell_1) - EI_3H'''_{23}(0)$;
$K_{14} = -EA_2h'_{22}(0)$; $K_{17} = EI_3H'''_{33}(0)$; $K_{19} = -EI_3H'''_{43}(0)$; $K_{1,10} = EA_4h'_{14}(\ell_4)$.
$K_{22} = EA_1h'_{22}(\ell_1,\omega) - EA_3h'_{13}(0) + EI_2H'''_{12}(0) - EI_4H'''_{34}(\ell_4) - m_1\omega^2$; $K_{23} = EI_2H'''_{22}(0) - EI_4H'''_4(\ell_4)$;
$K_{25} = EI_2H'''_3(0)$; $K_{26} = EI_2H'''_4(0)$; $K_{28} = -EA_3h'_2(0)$; $K_{2,11} = -EI_4H'''_1(\ell_4)$; $K_{2,12} = -EI_4H'''_{24}(\ell_4)$.
$K_{31} = EI_3H''_{13}(0) - EI_1H''_{31}(\ell_1)$; $K_{32} = EI_4H''_{34}(\ell_4) - EI_2H''_{12}(0)$; $K_{35} = -EI_2H''_{32}(0)$; $K_{36} = -EI_2H''_{42}(0)$;
$K_{33} = EI_1H''_{41}(\ell_1) - EI_2H''_{22}(0) - EI_3H''_{23}(0) + EI_4H''_{44}(\ell_4)$; $K_{37} = EI_3H''_{33}(0)$; $K_{39} = -EI_3H''_{43}(0)$;
$K_{3,11} = EI_4H''_{14}(\ell_4)$; $K_{3,12} = EI_4H''_{24}(\ell_4)$; $K_{41} = EA_2h'_{12}(\ell_2)$; $K_{45} = -EA_6h'_{26}(\ell_6)\sin\alpha_{26}\cos\alpha_{26}$;

$$K_{44} = EA_2h'_{22}(\ell_2) + EA_6h'_{26}(\ell_6)\cos\alpha_{26}\cos\alpha_{26} - m_2\omega^2\,;\quad K_{47} = EA_6h'_{16}(\ell_6)\cos\alpha_{26}\cos\alpha_{26}\,;$$
$$K_{48} = -EA_6h'_{16}(\ell_6)\sin\alpha_{26}\cos\alpha_{26}; K_{52} = -EI_2H'''_{12}(\ell_2);\ K_{53} = -EI_2H'''_{22}(\ell_2);$$
$$K_{57} = -EA_6h'_{16}(\ell_6)\sin\alpha_{26}\cos\alpha_{26}\,; K_{54} = -EA_6h'_{26}(\ell_6)\sin\alpha_{26}\cos\alpha_{26}\,;\ K_{56} = -EI_2H'''_{42}(\ell_2);$$
$$K_{55} = EA_6h'_{26}(\ell_6)\sin\alpha_{26}\sin\alpha_{26} - EI_2H'''_{32}(\ell_2) - m_2\omega^2;\ K_{58} = EA_6h'_{16}(\ell_6)\sin\alpha_{26}\sin\alpha_{26}\,;$$
$$K_{62} = EI_2H''_{12}(\ell_2); K_{63} = EI_2H''_{22}(\ell_2);\ K_{65} = EI_2H''_{32}(\ell_2); K_{66} = EI_2H''_{42}(\ell_2); K_{71} = -EI_3H'''_{13}(\ell_3);$$
$$K_{73} = EI_3H'''_{23}(\ell_3);\ \ K_{74} = -EA_6h'_{26}(0)\cos\alpha_{26}\cos\alpha_{26}; K_{75} = EA_6h'_{26}(0)\sin\alpha_{26}\cos\alpha_{26}\,;$$
$$K_{77} = EA_5h'_{25}(\ell_5)\cos\alpha_{45}\cos\alpha_{45} - EA_6h'_{16}(0)\cos\alpha_{26}\cos\alpha_{26} - EI_3H'''_{33}(\ell_3);$$
$$K_{78} = EA_5h'_{25}(\ell_5)\sin\alpha_{45}\cos\alpha_{45} + EA_6h'_{16}(0)\cos\alpha_{26}\sin\alpha_{26}\,;\ K_{79} = EI_3H'''_{43}(\ell_3);$$
$$K_{7,11} = EA_5h'_{15}(\ell_5)\cos\alpha_{45}\sin\alpha_{45}\,;\ K_{82} = EA_3h'_{13}(\ell_3); K_{84} = EA_6h'_{26}(0)\sin\alpha_{26}\cos\alpha_{26}\,;$$
$$K_{85} = -EA_6h'_{26}(0)\sin\alpha_{26}\sin\alpha_{26};\ \ K_{87} = EA_5h'_{25}(\ell_5)\sin\alpha_{45}\cos\alpha_{45} + EA_6h'_{16}(0)\sin\alpha_{26}\cos\alpha_{26}\,;$$
$$K_{88} = [EA_3h'_{23}(\ell_3) + EA_5h'_{25}(\ell_5)\sin\alpha_{45}\sin\alpha_{45} - EA_6h'_{16}(0)\sin\alpha_{26}\sin\alpha_{26}];$$
$$K_{8,10} = EA_5h'_{15}(\ell_5)\sin\alpha_{45}\cos\alpha_{45}\,;\ K_{8,11} = EA_5h'_{15}(\ell_5)\sin\alpha_{45}\sin\alpha_{45}$$
$$K_{91} = -EI_3H''_{13}(\ell_3);\ K_{93} = EI_3H''_{23}(\ell_3);\ K_{97} = -EI_3H''_{33}(\ell_3);\ K_{99} = EI_3H''_{43}(\ell_3).$$
$$K_{10,1} = -EA_4h'_{24}(0); K_{10,7} = -EA_5h'_{25}(0)\cos\alpha_{45}\cos\alpha_{45}\,; K_{10,8} = -EA_5h'_{25}(0)\cos\alpha_{45}\sin\alpha_{45}\,;$$
$$K_{10,11} = -EA_5h'_{15}(0)\cos\alpha_{45}\sin\alpha_{45}\,; K_{10,10} = -EA_5h'_{15}(0)\cos\alpha_{45}\cos\alpha_{45} - EA_4h'_{14}(0) - m_4\omega^2;$$
$$K_{11,2} = EI_4H'''_{34}(0);\ K_{11,3} = EI_4H'''_{44}(0);\ K_{11,7} = -EA_5h'_{25}(0)\sin\alpha_{45}\cos\alpha_{45}\,;$$
$$K_{11,8} = -EA_5h'_{25}(0)\sin\alpha_{45}\sin\alpha_{45}\,; K_{11,10} = -EA_5h'_{15}(0)\sin\alpha_{45}\cos\alpha_{45}\,;\ K_{11,12} = EI_4H'''_{24}(0).$$
$$\boldsymbol{K_{11,11} = EI_4H'''_{14}(0) - EA_5h'_{15}(0)\sin\alpha_{45}\sin\alpha_{45} - m_4\omega^2};$$
$$K_{12,2} = EI_4H''_{34}(0); K_{12,3} = EI_4H''_{44}(0); K_{12,11} = EI_4H''_{14}(0); K_{12,12} = EI_4H''_{24}(0),$$

where functions $h_{1k}(x), h_{1k}(x), k = 1,2,\dots,6$ and $H_{1j}(x), H_{2j}(x), H_{3j}(x), H_{4j}(x), j = 1,2,3,4$ are defined as follow

$$h_{1k}(x) = (1/d_k)\begin{vmatrix}\phi_1(x) & \phi_1(L_k)\\ \phi_4(x) & \phi_4(L_k)\end{vmatrix};\ h_{2k}(x) = (1/d_k)\begin{vmatrix}\phi_1(0) & \phi_1(x)\\ \phi_4(0) & \phi_4(x)\end{vmatrix};\ d_k = \begin{vmatrix}\phi_1(0) & \phi_1(L_k)\\ \phi_4(0) & \phi_4(L_k)\end{vmatrix};$$
$$\{H_{1j}(x), H_{2j}(x), H_{13}(x), H_{4j}(x)\}$$
$$= \{\phi_2(x), \phi_3(x), \phi_5(x), \phi_6(x)\}\begin{bmatrix}\phi_2(0) & \phi_3(0) & \phi_5(0) & \phi_6(0)\\ \phi'_2(0) & \phi'_3(0) & \phi'_5(0) & \phi'_6(0)\\ \phi_2(L_j) & \phi_3(L_j) & \phi_5(L_j) & \phi_6(L_j)\\ \phi'_2(L_j) & \phi'_3(L_j) & \phi'_5(L_j) & \phi'_6(L_j)\end{bmatrix}^{-1}$$

with functions $\phi_1(x), \dots, \phi_6(x)$ defined in (2.7).